J|A|C|S
ARTICLES
Published on Web 10/12/2006

# DFT Study on the Palladium-Catalyzed Allylation of Primary Amines by Allylic Alcohol

Olivier Piechaczyk, Claire Thoumazet, Yves Jean, and Pascal le Floch*

*Contribution from the Laboratoire "Hétéroéléments et Coordination", UMR CNRS 7653, Ecole Polytechnique, 91128 Palaiseau Cedex, France*

Received March 31, 2006; E-mail: lefloch@poly.polytechnique.fr

***Abstract:*** The palladium-catalyzed allylation of primary amines has been investigated by DFT calculations (B3PW91, PCM method), and two potential mechanisms were studied. The first mechanism relies on the formation of cationic hydridopalladium complexes. Their formation involves a metal-assisted formal (1,3) shift of a proton from the nitrogen atom of an ammonium to the C$\beta$ carbon atom. The second part of the cycle relies on a ligand exchange through a pentacoordinated 18VE hydridopalladium complex. The last step likely proceeds through a bimolecular pathway and formally consists of a proton transfer from the allylammonium to the alcohol group of the complex. The second mechanism, which is closer to that currently admitted for nucleophilic allylic substitutions, relies on the decomplexation of the coordinated allylammonium and appears to be favored. This catalytic cycle was recomputed on model complexes varying the ligands, and a charge decomposition analysis was carried out to assess the influence of the electronic properties of the ligands. To compare our results with competitive experiments, CDA calculations were also performed on real ligands. In agreement with experimental observations, this process was found to be strongly ligand dependent, decomplexation being favored by strong $\pi$-acceptor ligands. These calculations led us to show experimentally that complex [Pd(P(OPh)$_3$)$_2$($\eta^3$-C$_3$H$_5$)][OTf] is an efficient catalyst for this allylation. Finally, this catalytic process proved to be sensitive to the nature of the amine, with poorly basic amines favoring the re-formation of the catalytic precursor.

## Introduction

Transition metal-catalyzed processes that allow the formation of carbon−carbon and carbon−heteroatom (N, O, S) bonds are of utmost importance regarding their potential in organic chemistry for the synthesis of biologically active molecules.[1] Among various processes, allylic alkylations, which were discovered nearly three decades ago, are probably one of the most studied transformations because they involve reaction at a sp$^3$ hybridized carbon atom. Their utility in organic synthesis has been emphasized in several reviews. Although many metal centers (Ni, Pd, Pt, Mo, W, Ir, Ru)[2] have been shown to catalyze these transformations, most of the studies focused on the use of Pd(II) complexes, which proved to be the most active and versatile catalysts. The principle of this coupling mainly relies on the ability of the metal fragment to promote ionization of the leaving group on the allylic moiety to yield a transient ($\eta^3$-allyl) palladium complex, which then undergoes a nucleophilic attack on the coordinated allyl ligand. The catalytic cycle that is commonly admitted is presented in Scheme 1. Most of the mechanistical studies focus on either the elimination of the leaving group or the attack of the amine.[3]

In this process, the presence of a good leaving group (X) such as carboxylate, carbonate, phosphate, or other related derivatives on the allylic moiety is usually required because of the poor lability of the OH group. Although these allylic derivatives are easily available, an interesting challenge, from both an economical and an environmental point of view, would consist in directly employing allylic alcohols as substrates. This approach has not been thoroughly studied so far, but recent studies suggest that it can be done. Although some authors reported that activation of the OH group can be promoted by Lewis acids or by converting the alcohol into esters of inorganic

(1) (a) Trost, B. M. In *Advances in Natural Product Chemistry*; Atta-Ur-Rahman, Ed.; Harwood Academic Publishers: Harwood, 1992; pp 19−34. (b) Trost, B. M.; Crawley, M. L. *Chem. Rev.* **2003**, *103*, 2921−2943.

(2) (a) Muzart, J. *Tetrahedron* **2005**, *61*, 4179−4212. (b) Bricout, H.; Carpentier, J.-F.; Mortreux, A. *J. Mol. Catal. A* **1998**, *136*, 243−251. (c) Ohmura, T.; Hartwig, J. F. *J. Am. Chem. Soc.* **2002**, *124*, 15164−15165. (d) Godleski, S. A. In *Comprehensive Organic Synthesis*; Trost, B. M., Fleming, I., Eds.; Pergamon Press: New York, 1991; Vol. 4, pp 585−661. (e) Davis, J. A. In *Comprehensive Organometallic Chemistry II*; Abel, E. W., Stone, F. G. A., Wilkinson, G., Eds.; Pergamon: Oxford, 1995; Vol. 9, p 291. (f) Trost, B. M.; Toste, F. D.; Pinkerton, A. B. *Chem. Rev.* **2001**, *101*, 2067−2096. (g) Trost, B. M.; VanVranken, D. L. *Chem. Rev.* **1996**, *96*, 395−422. (h) Trost, B. M. *Acc. Chem. Res.* **1980**, *13*, 385−393. (i) Garcia-Yebra, C.; Janssen, J. P.; Rominger, F.; Helmchen, G. *Organometallics* **2004**, *23*, 5459−5470. (j) Glorius, F.; Pfaltz, A. *Org. Lett.* **1999**, *1*, 141−144. (k) Helmchen, G.; Pfaltz, A. *Acc. Chem. Res.* **2000**, *33*, 336−345. (l) Fuji, K.; Kinoshita, N.; Tanaka, K.; Kawabata, T. *Chem. Commun.* **1999**, 2289−2290. (m) Auburn, P. R.; Mackenzie, P. B.; Bosnich, B. *J. Am. Chem. Soc.* **1985**, *107*, 2033−2046.

(3) (a) Tang, D. Y.; Luo, X. L.; Shen, W.; Li, M. *J. Mol. Struct. (THEOCHEM)* **2005**, *716*, 79−87. (b) Amatore, C.; Gamez, S.; Jutand, A.; Meyer, G.; Moreno-Manas, M.; Morral, L.; Pleixats, R. *Chem.-Eur. J.* **2000**, *6*, 3372−3376. (c) Kollmar, M.; Steinhagen, H.; Janssen, J. P.; Goldfuss, B.; Malinovskaya, S. A.; Vazquez, J.; Rominger, F.; Helmchen, G. *Chem.-Eur. J.* **2002**, *8*, 3103−3114. (d) Kollmar, M.; Goldfuss, B.; Reggelin, M.; Rominger, F.; Helmchen, G. *Chem.-Eur. J.* **2001**, *7*, 4913−4927. (e) Dedieu, A. *Chem. Rev.* **2000**, *100*, 543−600. (f) Blochl, P. E.; Togni, A. *Organometallics* **1996**, *15*, 4125−4132. (g) Amatore, C.; Jutand, A.; Mensah, L.; Meyer, G.; Fiaud, J. C.; Legros, J. Y. *Eur. J. Org. Chem.* **2006**, 1185−1192. (h) Jutand, A. *Eur. J. Inorg. Chem.* **2003**, 2017−2040.



**10.1021/ja0621997 CCC: $33.50** 

***Scheme 1.*** Catalytic Cycle of the Nucleophilic Allylic Substitution

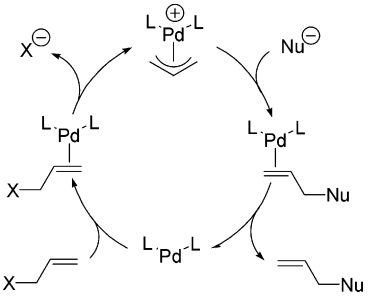

***Scheme 2.*** DPCB-Based Palladium Catalysts in the Amination of Allylic Alcohols

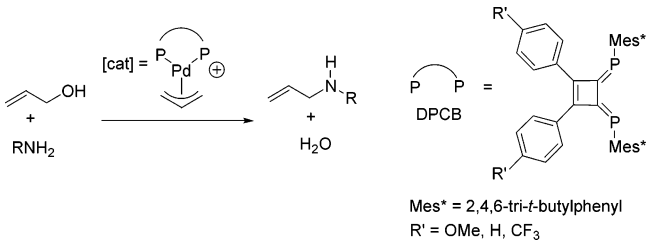


acids,[4] the most promising advance was reported by Ozawa and Yoshifuji. In 2002, they showed that (DPCB)($\eta^3$-allyl)Pd complexes (DPCB stands for diphosphinidenecyclobutene) could be used as efficient catalysts in the direct conversion of allylic alcohols into allylamines at room temperature (Scheme 2).[5] Importantly, in the same studies, they also showed that ($\eta^3$-allyl) palladium complexes featuring stronger donor ligands such as 1,4-diazabutadienes could not catalyze this process under the same experimental conditions.[6] Much more recently, we have shown that mixed ligands such as phosphabarrelene−phosphinosulfide could also be used efficiently in this allylation process.[7] Note that a common electronic property of both ligands is their $\pi$-accepting capacity.

So far, no theoretical mechanistic studies have been undertaken to rationalize this interesting coupling process. However, during their studies,[5,6,8] Ozawa and Yoshifuji suggested that the strong $\pi$-accepting capacity of DPCB ligands could accelerate the elimination of water from the transiently formed palladium−hydrido complex [Pd(DPCB)H($\eta^2$-$CH_2CHCH_2OH$)][OTf] **IIIa** to regenerate the catalytic precursor [Pd(DPCB)($\eta^3$-$C_3H_5$)][OTf] complex **Ia**. To support this proposal, they suggested that the hydrido complex [Pd(DPCB)H][OTf] complex **IIa**, which is the precursor of complex **IIIa**, could be transiently formed during the catalytic cycle (Scheme 3). This assumption was based upon the fact that the neutral [M(DPCB)(Me)OTf] **IVa** and **IVb** (**IVa**, M = Pd; **IVb**, M = Pt) complexes react with $HSiMe_2Ph$ in the presence of allylic alcohol to yield the corresponding cationic allyl complexes [M(DPCB)(allyl)][OTf] **Ia** and **Ib** (**Ia**, M = Pd; **Ib**, M = Pt) through elimination of one molecule of water. Although the hydrido species **IIa** and **IIb** were not detected in the reaction mixture, the isolation of the stable platinum dimer $[Pt(DPCB)H]_2[OTf]_2$ **Vb** furnished indirect evidence of their transient formation (at least in the case of platinum, see Scheme 4).

***Scheme 3.*** A Proposed Catalytic Cycle Involving Palladium Hydrido Species

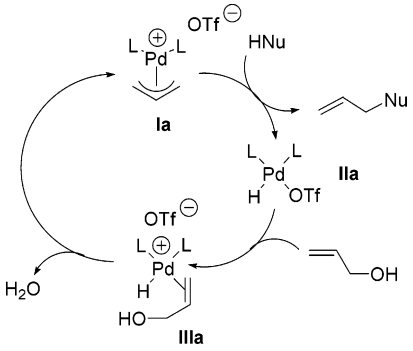


***Scheme 4.*** Reaction of Pd and Pt Hydrido Complexes with Allylic Alcohol

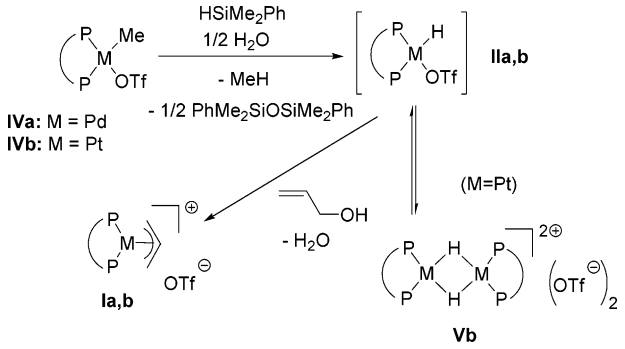


***Scheme 5.*** Formation of Complex **VIb**

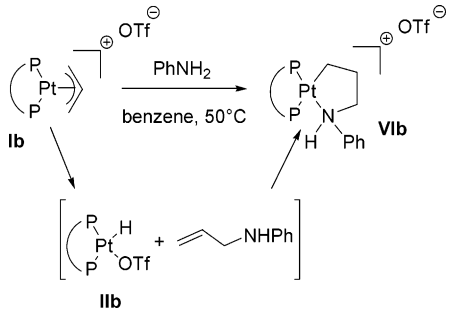


As can be seen in the following scheme, this elegant mechanism, which markedly differs from the commonly admitted one, relies on the possible formation of the hydrido complex **IIa**.

Additional evidence in favor of the formation of the cationic hydrido species was also given by the reaction of [Pt($\eta^3$-$C_3H_5$)-(DPCB)][OTf] complex **Ib** with aniline in benzene at 50 °C. It has been proposed that the resulting aminopropyl complex **VIb** could result from the transient formation of **IIb** (Scheme 5).[8]

The synthetic importance of this allylation process prompted us to shed some light on the possible mechanistic pathways. In this Article, we report on DFT calculations, which demonstrate that two mechanisms can be proposed. The first relies on the formation of palladium hydrido species, whereas the second, which is closer to the "classical" mechanism (Scheme 1), involves the decomplexation of an olefinic ligand. Importantly, these calculations also show that the electronic nature of the

(4) (a) Tamaru, Y. *Eur. J. Org. Chem.* **2005**, 2647−2656. (b) Tamaru, Y. *J. Organomet. Chem.* **1999**, *576*, 215−231. (c) Lu, X. Y.; Jiang, X. H.; Tao, X. C. *J. Organomet. Chem.* **1988**, *344*, 109−118. (d) Lu, X. Y.; Lu, L.; Sun, J. H. *J. Mol. Catal.* **1987**, *41*, 245−251.
(5) Ozawa, F.; Okamoto, H.; Kawagishi, S.; Yamamoto, S.; Minami, T.; Yoshifuji, M. *J. Am. Chem. Soc.* **2002**, *124*, 10968−10969.
(6) Ozawa, F.; Yoshifuji, M. *C. R. Chim.* **2004**, *7*, 747−754.
(7) Piechaczyk, O.; Doux, M.; Ricard, L.; Le Floch, P. *Organometallics* **2005**, *24*, 1204−1213.
(8) Ozawa, F.; Ishiyama, T.; Yamamoto, S.; Kawagishi, S.; Murakami, H.; Yoshifuji, M. *Organometallics* **2004**, *23*, 1698−1707.

***Scheme 6.*** Calculated Pathway for the Nucleophilic Attack of $MeNH_2$ on the Coordinated Allyl Ligand of Complex **1a**

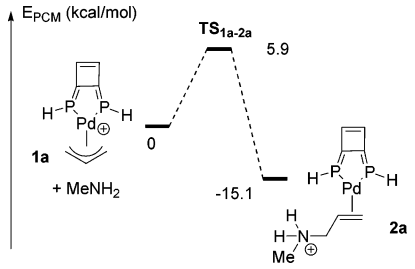


ligands plays a crucial role in the kinetics of the transformation and rationalize why strong $\pi$-acceptor ligands are well adapted for this catalytic transformation. Additional experiments have been undertaken to support this point. This theoretical study also led us to propose a very simple and efficient catalyst featuring triphenyl phosphite as ligand.

## Results and Discussion

**1. A First Proposal Based on the Transient Formation of Hydrido Species.** In a first step, we focused our calculations on the mechanism proposed by Ozawa and Yoshifuji. Calculations were carried out with the model ligand DPCB-H, in which the 2,4,6-tri-*tert*-butylphenyl groups (Mes*) on phosphorus and the phenyl groups on the four-membered cyclobutene ring have been replaced by hydrogen atoms. However, it is important to keep in mind that, in the real complex, the two Mes* groups at phosphorus sterically shield the coordination sphere of the palladium atom. In this first series of calculations, methylamine was used as a model of primary amine. All of these calculations were carried out using the Gaussian 03 set of programs with the B3PW91 functional, the 6-31+G* basis set for all nonmetallic atoms (H, C, O, N, P, F, S), and the Hay−Wadt basis set for palladium augmented with an f polarization function. Further computational details are given in the Experimental Section. To take into account the role of the solvent, single point calculations were carried out on the optimized structures using the polarized continuum model (PCM), THF being considered as the solvent. Several recent theoretical investigations indicate that continuum solvation models can be successfully applied to compute solvation free energies of neutral and ionic organic and inorganic molecules.[9] These models have also been used in mechanistic studies of organometallic reactions.[10]

The first step is the nucleophilic attack of the amine onto one of the terminal carbon atoms of the allyl ligand in complex **1a**. This reaction only requires a small activation energy as can be seen in Scheme 6 ($\Delta E_{PCM}^{\ddagger} = +5.9$ kcal/mol), and the formation of the cationic Pd(0) complex **2a** that features an $\eta^2$-coordinated allylammonium is thermodynamically favored ($E_{PCM} = -15.1$ kcal/mol). In all of our calculations, the reference ($E_{PCM} = 0$) corresponds to "complex **1a** + starting materials", and the energies of all other states take into account all of the molecules present. For the sake of clarity, only relevant molecules are considered in schemes and discussion. A view of the transition state $\mathbf{TS}_{1a-2a}$ is presented in Figure 1, and the most significant bond distances and bond angles are listed in the corresponding legend.

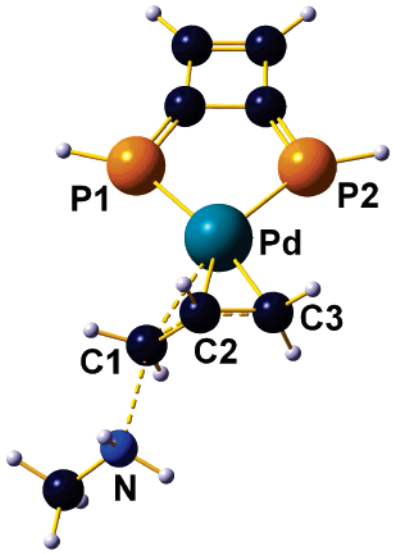


***Figure 1.*** View of the transition state $\mathbf{TS}_{1a-2a}$ connecting the two structures **1a** and **2a** as given by DFT calculations. Most significant bond distances (Å) and bond angles (deg): Pd−P1, 2.396; Pd−P2, 2.363; Pd−C1, 2.549; Pd−C2, 2.179; Pd−C3, 2.128; C1−N, 2.195; P1−Pd−P2, 84.6. Imaginary frequency at $-208$ cm$^{-1}$.

***Scheme 7.*** Possible Cationic Hydrido Complexes Formed from Complex **2a**

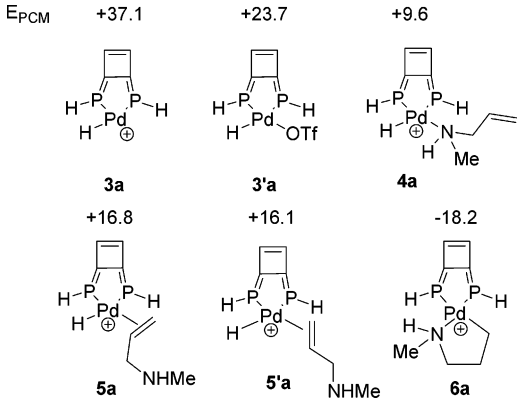


The second step of the mechanism proposed, which leads to the formation of the hydrido species, proved to be much more problematic to model. This hydrido complex was formulated as [Pd(DPCB)(H)(OTf)] by the authors, but no spectroscopic evidence was presented to support this formulation. It was assumed that this complex could be formed through an intramolecular hydrogen transfer from the ammonium to the palladium atom. Therefore, we decided to explore the PES (potential energy surface), and several structures were calculated (**3a**−**6a**, Scheme 7). Complex **3a** results from the intramolecular protonation of the palladium atom in complex **2a**, and the amine is supposed not to be coordinated on the palladium atom. Complex **3′a** is the triflate derivative of **3a** in which coordination of the triflate occurs through one oxygen atom. Complex **4a** formally results from the oxidative addition of the (DPCB-H)-Pd(0) fragment into one N−H bond of the allylammonium

(9) (a) Takano, Y.; Houk, K. N. *J. Chem. Theory Comput.* **2005**, *1*, 70−77. (b) Fu, Y.; Liu, L.; Li, R. C.; Liu, R.; Guo, Q. X. *J. Am. Chem. Soc.* **2004**, *126*, 814−822. (c) Baik, M. H.; Schauer, C. K.; Ziegler, T. *J. Am. Chem. Soc.* **2002**, *124*, 11167−11181. (d) Pliego, J. R.; Riveros, J. M. *J. Phys. Chem. A* **2002**, *106*, 7434−7439. (e) Lopez, X.; Schaefer, M.; Dejaegere, A.; Karplus, M. *J. Am. Chem. Soc.* **2002**, *124*, 5010−5018.

(10) (a) Nowroozi-Isfahani, T.; Musaev, D. G.; McDonald, F. E.; Morokuma, K. *Organometallics* **2005**, *24*, 2921−2929. (b) Marino, T.; Russo, N.; Toscano, M. *J. Am. Chem. Soc.* **2005**, *127*, 4242−4253. (c) Casey, C. P.; Johnson, J. B.; Singer, S. W.; Cui, Q. *J. Am. Chem. Soc.* **2005**, *127*, 3100−3109. (d) Schubert, G.; Papai, I. *J. Am. Chem. Soc.* **2003**, *125*, 14847−14858. (e) Kovacs, G.; Papai, I. *Organometallics* **2006**, *25*, 820−825.

***Scheme 8.*** Considered Mechanisms for the Formation of Complexes **5a** and **4a**

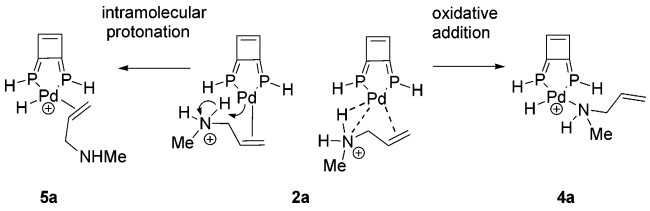


ligand. It was supposed that the resulting hydrido complex is stabilized by the coordination of the allylamine through the nitrogen atom. Complexes **5a** and **5′a** result from the intramolecular protonation of the (DPCB-H)Pd(0) fragment by the $NH_2^+$ moiety of the allylammonium. In these two complexes, the allylamine remains $\eta^2$-coordinated through the double bond. Two different conformations have been envisioned: one in which the olefin is located in the plane of the complex (**5a**) and the second in which it is located in a perpendicular plane (**5′a**). Finally, the last structure **6a** is the palladium analogue of the Pt complex **VIb**, which was experimentally characterized. Examination of relative energies shows that the formation of hydrido complexes **3a**−**5a** is endothermic. As expected, the coordinatively unsaturated complex **3a** is very high in energy ($E_{PCM}$ = +37.1 kcal/mol), and its formation is hardly conceivable under mild conditions. Among the other hydrido species, complex **4a** was found to be the most accessible ($E_{PCM}$ = +9.6 kcal/mol), complexes **5a** ($E_{PCM}$ = +16.8 kcal/mol) and **5′a** ($E_{PCM}$ = +16.1 kcal/mol) lying at higher energy. On the other hand, complex **3′a** was found to be the least stable 16VE hydrido complex ($E_{PCM}$ = +23.7 kcal/mol). Finally, the formation of complex **6a** appeared to be strongly favored on thermodynamical grounds ($E_{PCM}$ = −18.2 kcal/mol).

The transformations from complex **2a** to complexes **5a** and **4a** were then studied. Two mechanisms were considered, the direct transfer of one proton from the ammonium to the palladium center to form complex **5a** and the intramolecular oxidative addition of the tricoordinated 16VE Pd(0) fragment into one N−H bond to form **4a** (Scheme 8). Unfortunately, despite many attempts, no transition state could be located for these intramolecular processes.

However, a transition state connecting **2a** to the alkenyl complex **7a** was located. Complex **7a** is a cationic complex, which features an agostic bond between the hydrogen located on the C$\beta$ atom and the palladium atom. As compared to complexes **4a** and **5a**, **7a** is more accessible ($E_{PCM}$ = +5.8 kcal/mol), and we assumed that it could be the missing link in the transformation of **2a** into the hydrido species **5a**. Furthermore, the existence of complex **7a** could also rationalize the formation of complex **6a** through a simple intramolecular displacement reaction of ligands (Pd−H agostic to P−N bond). Because **6a** is energetically close to **2a** and is not an intermediate in the catalytic cycle, its formation will not be discussed any further. The transformation from **2a** to **7a** involves a (1,3)-shift of one proton of the ammonium to the C$\beta$ carbon atom of the olefin. As can be seen in Scheme 9 and in Figure 2 where the structure of $\mathbf{TS}_{2a-7a}$ is presented, this proton shift is assisted by the palladium atom. In $\mathbf{TS}_{2a-7a}$, the proton is connected to the nitrogen atom (2.035 Å), to the C$\beta$ carbon atom of the olefin (1.687 Å), and to the Pd atom (1.628 Å). This rearrangement

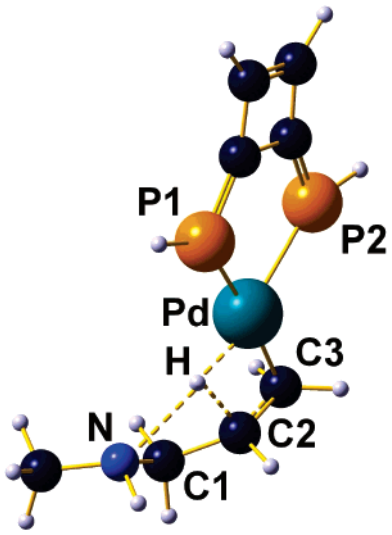


***Figure 2.*** View of the transition state $\mathbf{TS}_{2a-7a}$ connecting the two structures **2a** and **7a** as given by DFT calculations. Most significant bond distances (Å) and bond angles (deg): Pd−P1, 2.354; Pd−P2, 2.409; Pd−H, 1.628; Pd−C3, 2.147; C3−C2, 1.407; C2−H, 1.687; H−N, 2.035; P1−Pd−P2, 84.1; Pd−C3−C2, 76.8; C3−C2−H, 111.0. Imaginary frequency at −404 $cm^{-1}$.

***Scheme 9.*** Calculated Pathway for the Transformation of **2a** into **7a**

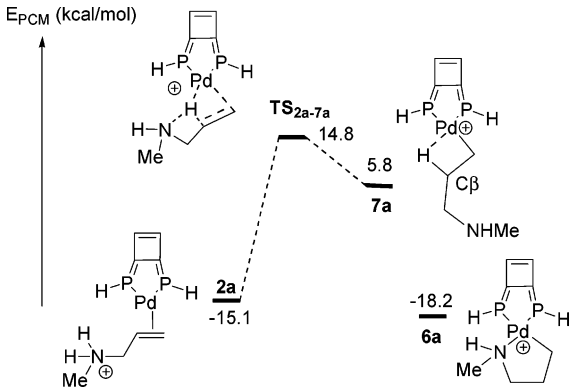


requires an activation energy of $\Delta E_{PCM}^{\ddagger}$ = +29.9 kcal/mol (Scheme 9), and $\mathbf{TS}_{2a-7a}$ lies at lower energy than do complexes **5a** and **5′a**.

It is important to mention that this type of rearrangement is not totally unprecedented and, in 2000, Senn et al.[11] reported a similar transformation in their ab initio DFT studies of Co, Rh, Ni, Pd, and Pt alkene hydroamination catalysts. In their study, they showed that $[M(PH_3)_2(Cl)CH_2CH_2NH_3]^{n+}$ complexes rearrange into $[M(PH_3)_2(Cl)]^{n+}$ complexes with the concomitant release of one molecule of ethylamine. In the case of group 10 metals (Scheme 10), this process proceeds via protonolysis of the metal−carbon bond involving a M−($\mu$-H)−C bridged transition state. This mechanism was shown to be favored in the case of group 10 metals, whereas it leads to hydride intermediates for group 9 metals.

Formation of complex **5a** from **7a** relies on a classical $\beta$ elimination process, which requires an activation energy of $\Delta E_{PCM}^{\ddagger}$ = 11.0 kcal/mol. Our calculations showed that this process is highly endothermic because the structure of $\mathbf{TS}_{7a-5a}$ is very close to that of **5a**. Considering the precision of our

(11) Senn, H. M.; Blochl, P. E.; Togni, A. *J. Am. Chem. Soc.* **2000**, *122*, 4098−4107.

***Scheme 10.*** Cleavage through Protonolysis of a Metal−Carbon Bond in Group 10-Catalyzed Amination Processes

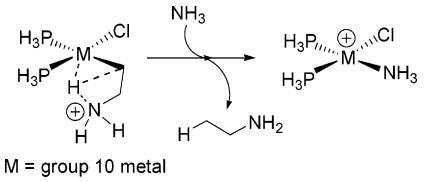


***Scheme 11.*** Calculated Pathway for the Transformation of **7a** into **5a** and **5′a**

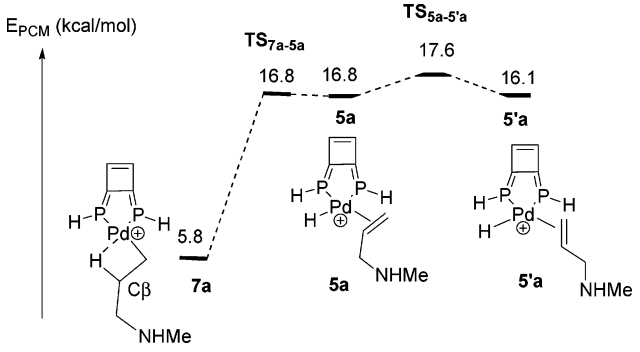


calculations, both structures are equivalent from an energetic point of view ($E_{PCM}$ = 16.8 kcal/mol). However, **TS**$_{7a-5a}$ was characterized by one imaginary frequency, whereas **5a** is a local minimum. The formation of **5′a** is easily explained by considering a simple rotation of the olefin around the axis connecting the Pd atom to the centroid of the olefinic ligand. A small activation energy is needed ($\Delta E_{PCM}^{\ddagger}$ = +0.8 kcal/mol), and **TS**$_{5a-5'a}$ (one imaginary frequency at −20 cm$^{-1}$) was found to be very close in energy to complex **5′a** (Scheme 11).

Having discovered a possible pathway explaining the formation of the hydrido species **5a** and **5′a**, we then turned our attention to the second part of the mechanism, which involves the release of the allylamine and the re-formation of the starting precursor, complex **1a**, through the transient formation of complex **9a**, which features an $\eta^2$-coordinated molecule of allylic alcohol. Two pathways were studied: a dissociative and an associative pathway. The former can be ruled out because it involves the formation of the d$^8$ 14VE complex **3a**, which lies at relatively high energy ($E_{PCM}$ = +37.1 kcal/mol). No transition state could be characterized when we examined the transformation yielding complex **9a** from complex **5a**. Each attempt yielded the pentacoordinated 18VE complex **8a** in which the two olefinic ligands are $\eta^2$-coordinated as a minimum. As can be seen in Scheme 12, this complex lies slightly higher in energy than do complexes **5a** and **5′a** ($E_{PCM}$ = +18.9 kcal/mol). It is important to keep in mind that the coordination sphere of the palladium is probably hardly accessible due to the presence of Mes* groups on each phosphorus atoms, especially for **8a**, which is a pentacoordinated complex. Therefore, the formation of such a 18VE complex is likely to be disfavored. This point will be discussed later in the case of ONIOM calculations. However, if these steric constraints are not considered, we can reasonably propose that the decoordination of one molecule of allylamine can yield complex **9a**.

As was shown experimentally by Ozawa and Yoshifuji, re-formation of the cationic ($\eta^3$-allyl) palladium complex **1a** from a species such as **9a** should be realistic.[8] In good agreement with these experimental data, we found that the transformation

***Scheme 12.*** Calculated Pathway for the Transformation of **5a** into **9a** through the Formation of 18VE Complex **8a**

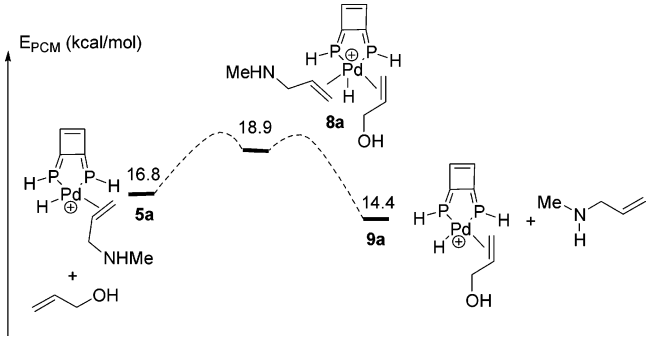


***Scheme 13.*** Calculated Pathway for the Transformation of **9a** into **1a** through Direct Elimination of Water

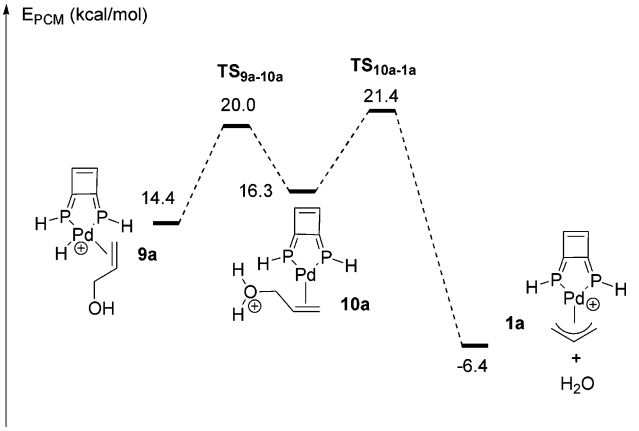


from **9a** to **1a** is strongly thermodynamically favored. This transformation does not proceed through a single step, and the transient formation of complex **10a** occurs. This complex results from the transfer of the hydride onto the OH group of the coordinated alcohol. Note that this transfer does not require a large activation energy ($\Delta E_{PCM}^{\ddagger}$ = 5.6 kcal/mol). The second step, which yields one molecule of water and complex **1a**, is comparable in terms of activation energy ($\Delta E_{PCM}^{\ddagger}$ = 5.1 kcal/mol). All of these results are summarized in Scheme 13.

Although this mechanism is perfectly conceivable both from a kinetic and from a thermodynamic point of view, it probably cannot account for the formation of complex **1a**. Indeed, one must keep in mind that allylamine as well as methylamine are present in the reaction medium and, considering the respective basicity of alcohols and primary amines, a base-assisted deprotonation of the protonated alcohol should be more realistic. As can be expected, geometry optimization of the adduct between complex **10a** and methylallylamine yielded a thermodynamically favored adduct **11a** in which the proton has been transferred to the nitrogen atom but remains in interaction with the oxygen atom of the coordinated allylic alcohol (Scheme 14). The second step of the mechanism involves the release of one molecule of water, methylallylamine, and complex **1a** ($\Delta E_{PCM}^{\ddagger}$ = 21.7 kcal/mol).[12] Although this last transformation is kinetically less favored than the elimination of water from complex **10a**, we believe that this second mechanism is more realistic (note that the same activation energy is needed when the

(12) The assistance of molecules of water has been proposed in the literature and is supported by DFT calculations, see: Kinoshita, H.; Shinokubo, H.; Oshima, K. *Org. Lett.* **2004**, *6*, 4085−4088.

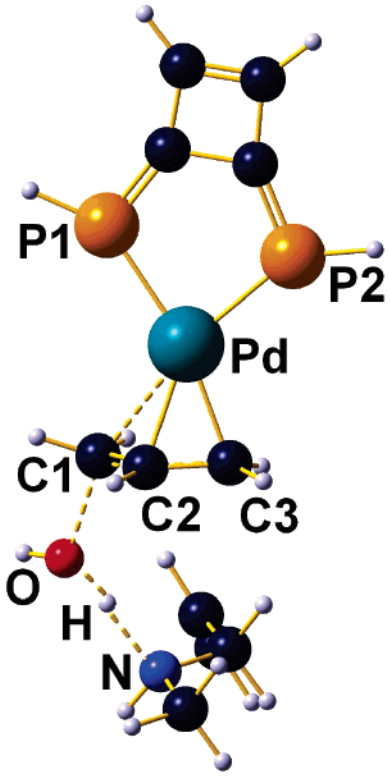


***Figure 3.*** View of transition state $\mathbf{TS}_{11a-1a}$. Most significant bond distances (Å) and bond angles (deg): Pd−P1, 2.396; Pd−P2, 2.366; Pd−C1, 2.695; Pd−C2, 2.176; Pd−C3, 2.119; C1−O, 1.899; O−H, 1.090; H−N, 1.488; P1−Pd−P2, 84.5. Imaginary frequency at −336 $cm^{-1}$.

***Scheme 14.*** Formation of Adduct **11a** and Elimination of Water and Methylallylamine

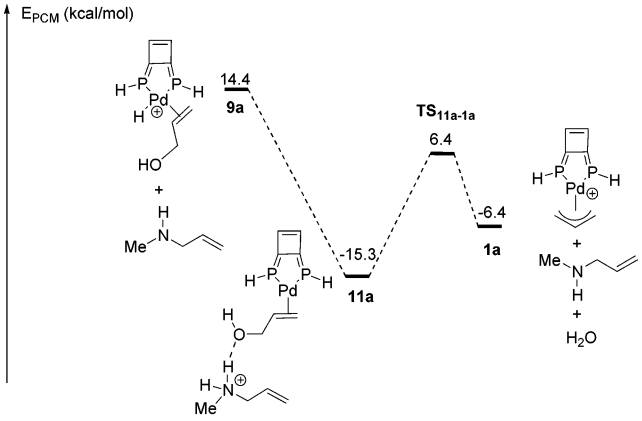


assistance of the methylamine instead of the methylallylamine is considered). A view of transition state $\mathbf{TS}_{11a-1a}$ is presented in Figure 3, and the most relevant theoretical metric parameters are listed in the corresponding legend.

This first part of the study shows that a mechanism involving the transient formation of hydrido species can be proposed, although complexes **5a**, **8a**, **9a**, and **10a** are relatively high in energy with respect to **2a**. Most importantly, this mechanism is consistent with the fact that hydrido complexes such as **9a** can constitute efficient precursors of ($\eta^3$-allyl) palladium complexes such as **1a** in the presence of allylic alcohols. In the following scheme, the different steps of the catalytic cycle computed in the case of the model DPCB-H ligand are summarized (Scheme 15).

***Scheme 15.*** Calculated Pathway for the Complete Catalytic Cycle Involving Hydrido Species

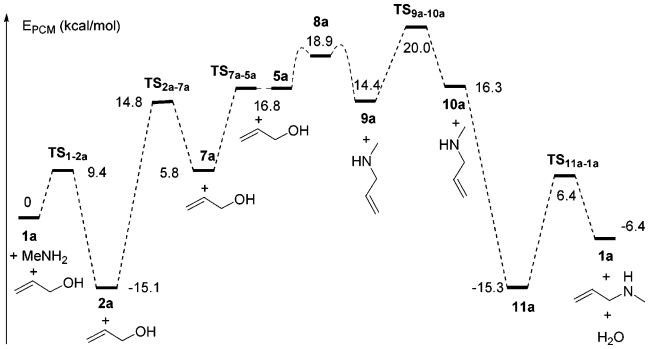


***Scheme 16.*** Dissociation of Methylallylammonium from **2a** and Recoordination of Allyl Alcohol from **12a** To Yield **13a**

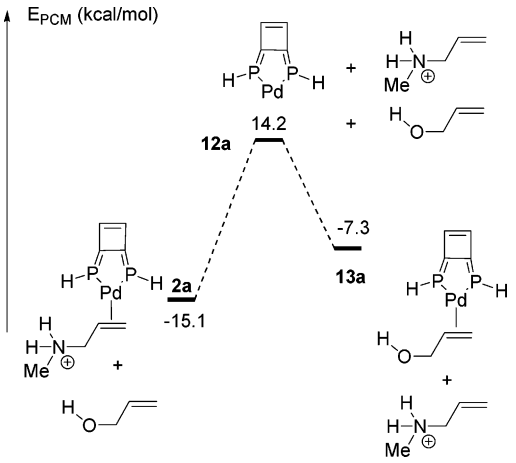


**2. A Second Proposal Involving the Decomplexation of the Allylammonium Ligand.** To find an alternative to the formation of the hydrido species, we explored pathways that can explain the transformation of complex **2a** into complex **11a**, these two species being low-lying in energy. We focused our attention on a classical dissociative pathway in which the transient 14VE [Pd(DPCB-H)] complex **12a** is formed. Interestingly, we found that complex **12a** only lies at 14.2 kcal/mol. Importantly, we also found that the formation of the tricoordinated 16VE Pd(0) complex [Pd(DPCB−)($\eta^2$-$HOCH_2$–CH═$CH_2$)] **13a** from **12a** and one molecule of allylic alcohol is thermodynamically favored as expected ($E_{PCM}$ = −7.3 kcal/mol), contrary to that of the corresponding hydrido complex **9a** ($E_{PCM}$ = 14.4 kcal/mol) (Scheme 16).

Some experimental evidence supporting this proposal was recently presented by Hartwig et al.[13] In 2006, in a study on the Pd-catalyzed hydroamination of olefins, they showed that reaction of a cationic ($\eta^3$-allyl) palladium complex with aniline affords transiently a 14VE species. Convincing evidence was given by the trapping of the 14VE fragment [$PdL_2$] with phenylacetylene (Scheme 17).

The end of the mechanism is analogous to that formally discussed with hydrido species. Indeed, **13a** is very unlikely to regenerate **1a** by direct elimination of $OH^-$. Taking into account the presence of the allylammonium in the reaction mixture, we considered the coordination of one lone pair at the oxygen atom by a proton of the allylammonium to afford complex **11a**. This

(13) Johns, A. M.; Utsunomiya, M.; Incarvito, C. D.; Hartwig, J. F. *J. Am. Chem. Soc.* **2006**, *128*, 1828−1839.

***Scheme 17.*** Evidence for the Formation of a 14VE Complex in the Reaction of Aniline with a Pd(allyl) Complex

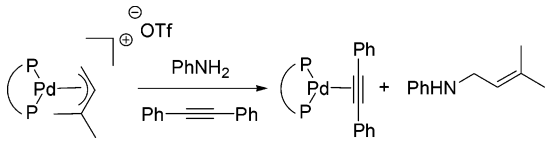


***Scheme 18.*** Re-formation of Complex **1a** from Complex **13a**

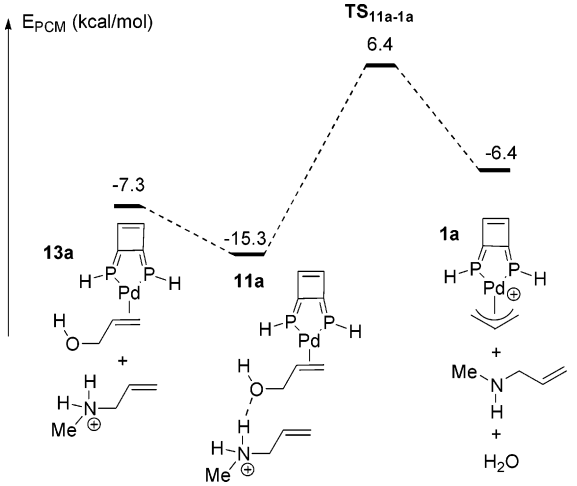


***Scheme 19.*** Comparison of the Two Calculated Catalytic Cycles (Mechanism Involving Hydrido Complexes Is Represented in Dotted Lines)

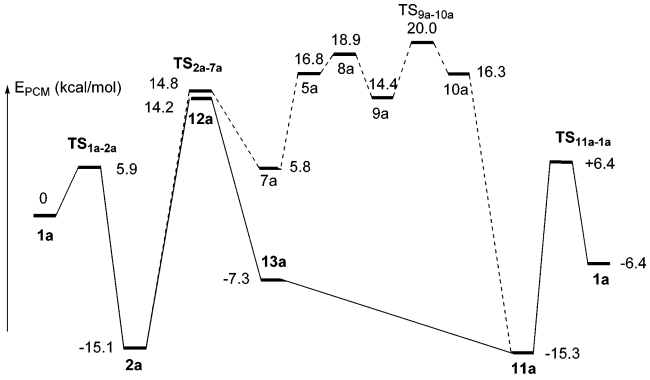


aggregate can release one molecule of water and the free methylallylamine to afford complex **1a** ($\Delta E_{PCM}^{\ddagger} = 21.7$ kcal/mol) (Scheme 18).

A new mechanism can therefore be proposed. Note that this cycle is closer to the currently admitted mechanism proposed for the Tsuji−Trost process. At first sight, it is not particularly evident to draw a definitive conclusion. Nevertheless, much evidence supports this second mechanism. The overall activation energy is 6 kcal/mol higher for the first mechanism if only the highest and the lowest states of both cycles are considered ($\Delta E_{PCM}^{\ddagger} = 35.3$ kcal/mol vs $\Delta E_{PCM}^{\ddagger} = 29.5$ kcal/mol). In both cases, the rate-determining step requires similar activation energy, but in the first case, the following hydrido species remain high in energy and all steps are reversible. In the second case, the coordination of the allyl alcohol leads to a stabilized state, which can easily undergo elimination of water assisted by the ammonium. The two pathways are gathered in Scheme 19.

Moreover, it is important to keep in mind that the formation of encumbered complexes such as **5a**, **5a′**, **8a**, or **9a** would be disfavored because of the steric crowding brought by the two Mes* groups. In this context, **8a** should be the most destabilized species as it is a pentacoordinated complex. Because it is already the highest local minimum, complex **8a** will be the species considered in the comparison between the two mechanisms on fully substituted complexes. The key species in both mechanisms (**8ar** and **12ar**, r meaning real) were computed on the fully substituted complexes. Geometry optimizations were carried out using the hybrid ONIOM method (B3PW91/UFF). The phenyl groups of Mes* on the phosphorus atoms were calculated at the quantum level; the tertiobutyl substituents of the Mes* groups as well as the two phenyl substituents of the cyclobutene ring were optimized at the MM level (Scheme 20). Single point PCM calculations were performed on these optimized geometries at the quantum level (Scheme 21). In the calculations on the model complexes, **8a** and **12a** were of comparable energy ($E_{PCM}$(**8a**) − $E_{PCM}$(**12a**) = 4.7 kcal/mol), whereas calculations on the fully substituted complexes lead to very different states, **8ar** being notably disfavored ($E_{PCM}$(**8ar**) − $E_{PCM}$(**12ar**) = 14.4 kcal/mol). This additional result enables us to exclude the first mechanism and favor the mechanism proceeding through the formation of 14VE Pd(0) complexes.

On the ground of these results, one can logically wonder why the bicyclic palladium complex **6a** is not observed whereas it was isolated with platinum. This raises the problem of the direct comparison between transition metals of the second and the third

***Scheme 20.*** Calculated Fully Substituted Complexes (Atoms Computed at the MM Level of Theory Are Represented in Gray)

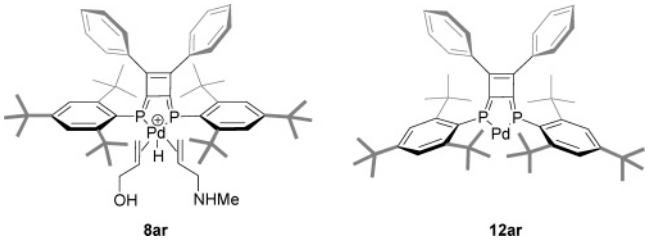


***Scheme 21.*** First Steps of Both Mechanisms with Platinum: Explanation of the Formation of Complex **17a**

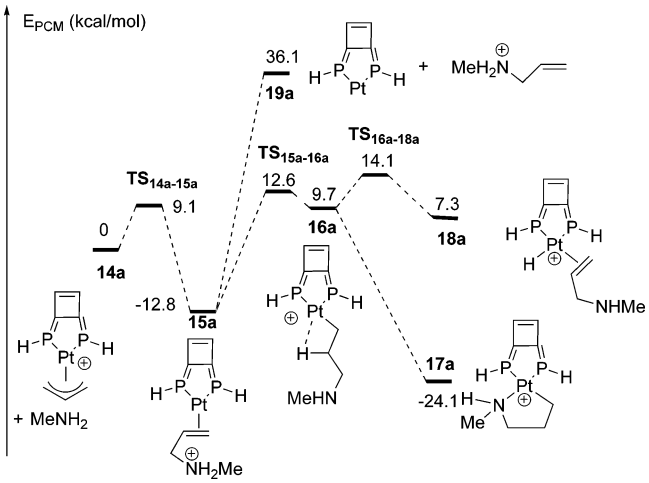


***Scheme 22.*** Model Complexes

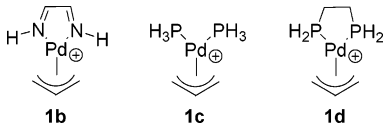

***Scheme 23.*** Calculated Pathways with Different Model Complexes

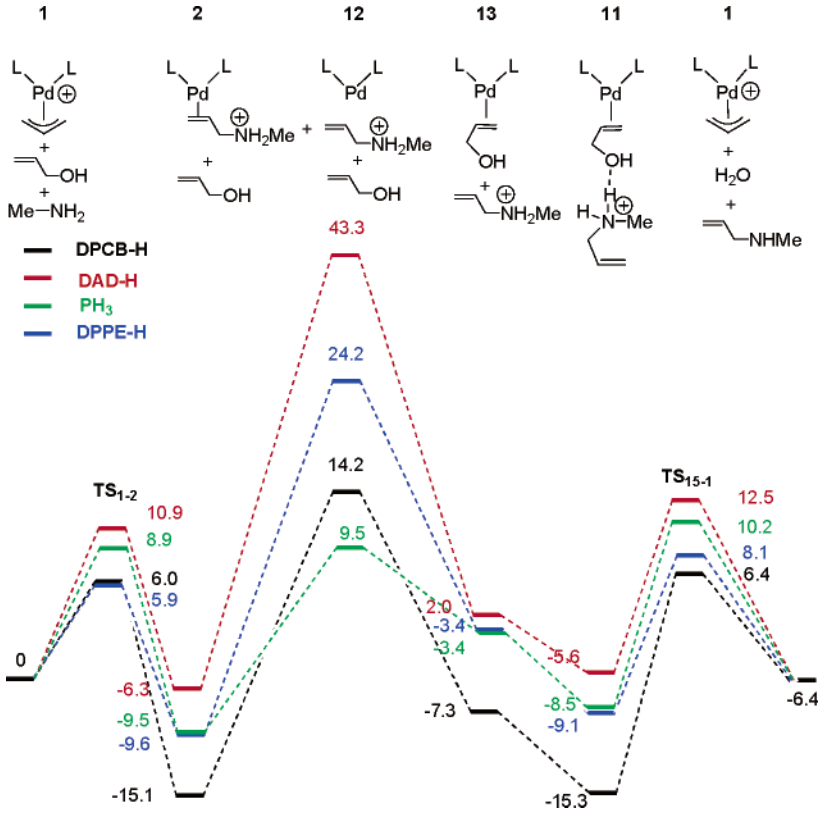


rows. Therefore, to complete our analysis, we computed the first steps of the two mechanisms when platinum is used as metal (Scheme 21).

First, it appears that the activation energy needed for the nucleophilic attack of the coordinated allyl ligand (from **14a** to **15a**) compares to that of Pd-catalyzed process. However, in line with Yoshifuji and Ozawa's experimental observation, the formation of complex **17a** (the Pt analogue of complex **6a**) is thermodynamically favored with regards to its palladium counterpart ($E_{PCM} = -24.1$ kcal/mol for Pt as compared to $E_{PCM} = -18.2$ kcal/mol for Pd). This is in agreement with thermodynamical data, which show that bondings involving platinum are energetically stronger than those involving palladium.[14] Thus, in the case of platinum, complex **17a** behaves as a thermodynamic sink, and the formation of complex **18a** that would allow it to enter the catalytic cycle is strongly disfavored. Moreover, it is evident that the dissociation step that leads to complex **19a** and free allylammonium is hardly conceivable ($\Delta E_{PCM}^{\ddagger} = 48.9$ kcal/mol). As will be seen further, this can be easily explained when the importance of the $\pi$-back-bonding in **15a** is taken into account.

**3. Influence of the Ligands.** The second mechanism being favored, we turned our attention onto ligand effects. As stated in the Introduction, DPCB ligands are known to act as strong $\pi$-acceptor ligands like other low coordinated phosphorus derivatives,[15] and this electronic property seems to be linked to its remarkable activity in this process. Therefore, the whole catalytic cycle was computed varying the nature of the ligands. Complex **1b** [Pd(DAD-H)($\eta^3$-allyl)$^+$] features the parent 1,4-diazadiene as a prototype of good donor ligands. Complex **1d**

(14) Simoes, J. A. M.; Beauchamp, J. L. *Chem. Rev.* **1990**, *90*, 629−688.
(15) Le Floch, P. *Coord. Chem. Rev.* **2006**, *250*, 627−681.

***Scheme 24.*** Principle of the CDA Analysis in Complexes **2**

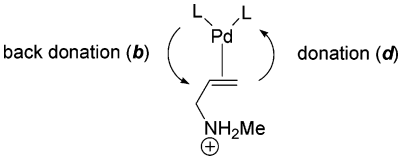


is the $H_2PCH_2CH_2PH_2$ (DPPE-H) derivative [Pd(DPPE-H)($\eta^3$-allyl)$^+$] and is expected to exhibit intermediate electronic properties (between DCPB-H and DAD-H), and complex **1c**, which features the monodentate $PH_3$ ligand [Pd($PH_3$)$_2$($\eta^3$-allyl)$^+$], has been chosen to probe the influence of the chelate effect (Scheme 22).

The different computed pathways are presented in Scheme 23. It appears that the first step (nucleophilic attack) is ligand dependent. Thus, a good donor ligand such as diazadiene makes the process less thermodynamically favored. On the contrary, in the case of strong $\pi$-acceptor ligands, the formation of complex **2** is more exothermic ($E_{PCM} = -6.3$ kcal/mol for DAD-H and $-15.1$ kcal/mol in the case of DPCB-H). The second step is calculated to be the kinetically determining step in each case. As can be seen, the use of good donor ligands such as DAD-H does not favor the formation of the 14VE palladium species ($E_{PCM} = 43.3$ kcal/mol for DAD-H and 14.2 kcal/mol for DPCB-H). This information is consistent with experimental observations. From these data, it also appears that the dissociation of the allylammonium from the DPPE-H complex requires a significant energy ($\Delta E_{PCM} = 33.8$ kcal/mol), while it is easier for the $PH_3$ complex ($\Delta E_{PCM} = 19.0$ kcal/mol). For all other steps, $PH_3$ and DPPE-H behave similarly. The difference of endothermicity in this dissociation step probably results from a change in the geometry. Indeed, the geometry optimized for the 14VE complex **12c** is found to be

***Table 1.*** Analysis of Complexes **2** Using the CDA Program[a]

| complex | *d* | *b* | *b*/*d* | *b*/(*d* + *b*) | *r* | Δ | *d*(C═C) |
|---|---|---|---|---|---|---|---|
| **2a**:DPCB-H | 0.453 | 0.370 | 0.82 | 45.0% | −0.161 | −0.004 | 1.417 |
| **2b**:DAD-H | 0.496 | 0.468 | 0.94 | 48.5% | −0.160 | −0.019 | 1.436 |
| **2c**:$PH_3$ | 0.461 | 0.390 | 0.85 | 45.9% | −0.167 | −0.004 | 1.419 |
| **2d**:DPPE-H | 0.474 | 0.401 | 0.85 | 45.8% | −0.161 | −0.007 | 1.425 |
| **15a**:Pt | 0.363 | 0.438 | 1.2 | 54.7% | −0.265 | −0.008 | 1.451 |

[a] *d* represents donation (expressed in e), *b* represents back-donation (expressed in e), *r* represents repulsion (expressed in e), and Δ represents residual (expressed in e). C═C bond distances are given in angstroms.

linear, whereas its DPPE-H counterpart **12d** is forced to remain bent. On the contrary, the last step (elimination of water, allylamine, and re-formation of complex **1**) seems to be slightly favored when donor ligands are used ($\Delta E_{PCM}$ = 18.1 kcal/mol for DAD-H and $\Delta E_{PCM}$ = 21.7 kcal/mol for DPCB-H).

These results led us to thoroughly investigate the second step of the mechanism, which corresponds to the dissociation of the olefin. The activation energy needed to achieve the dissociation is linked to the strength of the Pd−olefin bond. Considering the currently admitted Dewar−Chatt−Duncanson model,[16] this bond strength is linked to the electronic properties of the ligands on the Pd atom: the more electron-rich is the metal, the more efficient is the $\pi$-back-donation and consequently there is a stronger Pd−olefin bond. Thus, complexes bearing strong electron donor ligands should require a higher activation energy to dissociate the olefin. To quantify the electronic exchange between the metal fragment [$PdL_2$] and the allylammonium ligand in complexes **2**, a charge decomposition analysis using the CDA program developed by the group of Frenking[17,18] was carried out. This type of analysis already proved to be highly relevant to analyze the ratio between donation and back-donation in transition metal complexes featuring different types of 2e donor ligands. Further details on the method are given in the Supporting Information. In a first series of calculations, we focused on model complexes **2**, and the amount of $\pi$-back-bonding in the $\pi$* system of the olefin was quantified. The complex was divided into two fragments, the [$PdL_2$] donor fragment and the coordinated allylammonium, which was considered as the acceptor fragment (Scheme 24). All of these results are summarized in Table 1. As can be seen, all of the residual terms (Δ) are close to zero, which is a prerequisite for the analysis to be relevant in terms of donor−acceptor interaction following the Dewar−Chatt−Duncanson model. In this table are also reported values of the C−C bond length of the coordinated allylammonium. Interestingly, there is a good correlation between *b*/*d* ratio and this C−C bond distance, the stronger donor ligands leading to the greater lengthening of the bond (better $\pi$-back-donation). These data match the dissociation energies presented in Scheme 23. The most efficient donor, the [(DAD-H)Pd] fragment (*b*/*d* = 0.94), leads to the most difficult dissociation, followed by the [(DPPE-H)Pd] (*b*/*d* = 0.85), and finally the [(DPCB-H)Pd] (*b*/*d* = 0.82), which is the most accepting, gives an easier dissociation. The only exception is found for the [$(PH_3)_2$Pd] fragment (*b*/*d* = 0.85) where the dissociation energy is less important than for [(DPPE-H)Pd], while they seem electronically equivalent. However, as previously explained, care must be taken because the dissociation of these complexes leads to fragments of different geometries (linear fragment for **12c**). Even though the differences of *b*/*d* ratio are small, they are correlated to significant energetic changes, and CDA calculations enable one to predict the outcome of the dissociation step with good accuracy. Analogous CDA calculations were performed on the platinum complex **15a**, and, as previously mentioned, a very important $\pi$-back-donation occurs (*b*/*d* = 1.2) corresponding to a large dissociation energy ($\Delta E_{PCM}$ = 48.9 kcal/mol). Therefore, in this case, dissociation cannot occur under the experimental conditions.

To complete our study, we considered carrying out competitive experiments. Indeed, we wondered how relevant model ligands are compared to fully substituted ligands on electronic grounds to predict the catalytic activities of their palladium complexes. Similar CDA calculations were performed on the real complexes to compare the results with experiments. As was previously described, **2ar** has been optimized using the hybrid ONIOM method (B3PW91/UFF). Similar calculations were carried out for **2br** (DAD) where the two phenyl groups were computed at the quantum level and the isopropyl substituents

***Scheme 25.*** Calculated Real Molecules (Atoms Computed at the MM Level of Theory Are Represented in Gray)

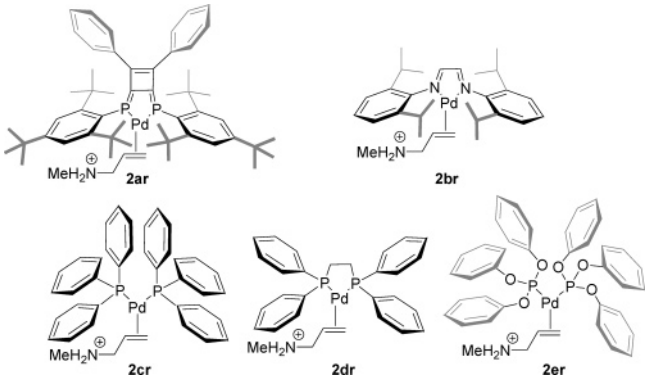


***Table 2.*** Analysis of Complexes **2r** (on Geometries Optimized by ONIOM Calculations) Using the CDA Program[a]

| complexes | *d* | *b* | *b*/*d* | *b*/(*d* + *b*) | *r* | Δ | *d*(C═C) |
|---|---|---|---|---|---|---|---|
| **2ar**:DPCB | 0.521 | 0.408 | 0.78 | 43.9% | −0.180 | 0.000 | 1.422 |
| **2br**:DAD | 0.555 | 0.459 | 0.83 | 45.3% | −0.179 | −0.011 | 1.435 |
| **2cr**:$PPh_3$ | 0.536 | 0.442 | 0.82 | 45.2% | −0.198 | 0.001 | 1.424 |
| **2dr**:DPPE | 0.497 | 0.422 | 0.85 | 45.9% | −0.171 | −0.004 | 1.433 |
| **2er**:$P(OPh)_3$ | 0.527 | 0.397 | 0.75 | 43.0% | −0.187 | −0.001 | 1.412 |

[a] *d* represents donation (expressed in e), *b* represents back-donation (expressed in e), *r* represents repulsion (expressed in e), and Δ represents residual (expressed in e). C═C bond distances are given in angstroms.

***Table 3.*** Catalytic Results in the Allylic Amination of Aniline with Complexes **1br**, **1cr**, **1dr**, and **1er** in THF (Conversions Determined by GC)

| catalyst | counterion | temperature | 24 h | 1 h |
|---|---|---|---|---|
| **1br** | OTf | rt | 0% | NT |
| | OTf | 50 °C | 20% | NT |
| **1dr** | OTf | rt | 5% | NT |
| | OTf | 50 °C | 20% | NT |
| **1cr** | OTf | rt | 100% | 47% |
| **1er** | OTf | rt | 100% | 76% |
| | $BF_4$ | rt | 100% | 76% |

***Scheme 26.*** Palladium-Catalyzed Allylic Amination of Aniline with Complexes **1br**, **1cr**, **1dr**, and **1er** in THF

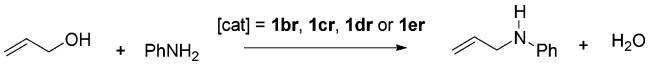


(16) Chatt, J.; Duncanson, L. A. *J. Chem. Soc.* **1953**, 2939−2947.
(17) Frenking, G.; Frohlich, N. *Chem. Rev.* **2000**, *100*, 717−774.
(18) Dapprich, S.; Frenking, G. *J. Phys. Chem.* **1995**, *99*, 9352−9362.

***Scheme 27.*** Calculated Pathways for the Allylation of Aniline and Methylamine Catalyzed by Complex **2a**

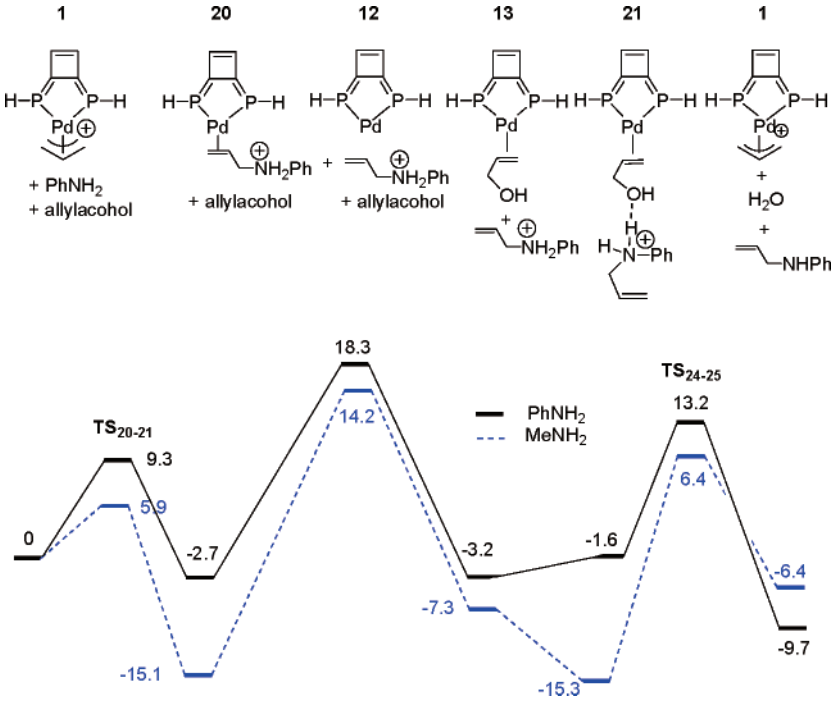


at the MM level. Complexes **2cr** and **2dr** were optimized at the quantum level. Phosphites being known as strong $\pi$-acceptor ligands, we enlarged our analysis to the triphenyl phosphite derivative **2er**. In this complex, the six phenyl groups that are not directly bound to the phosphorus atom were modelized at the MM level of theory (Scheme 25). These optimizations were followed by population analysis at the quantum level for all atoms. All of the results of the CDA calculations are presented in Table 2.

As can be seen, a comparison with data recorded for the models shows that care must be taken in replacing substituents by hydrogen atoms. Indeed, considering real complexes leads to notable variations especially for ligand **2br**, which is not as much of a donor as its model ($b/d$ = 0.83 for **2br** vs $b/d$ = 0.94 for model **2b**), and compare with **2dr** ($b/d$ = 0.85). **2ar** also appears to be more of an acceptor than its model **2a** ($b/d$ = 0.78 for **2ar** vs $b/d$ = 0.82 for **2a**). From these data, we can deduce that diazadiene (**2br**) and DPPE (**2dr**) should behave similarly. On the other hand, DPCB (**2ar**) and $P(OPh)_3$ (**2er**, $b/d$ = 0.75) are found to be relatively close if we examine the $b/d$ ratio, and therefore **2er** is expected to display good activity in this palladium-catalyzed process. Here again, we believe that no definitive conclusion can be drawn for $PPh_3$. According to these data, $PPh_3$ (**2cr**, $b/d$ = 0.82) should compare with DPPE (**2dr**) and DAD (**2br**), but, in practice, one may expect a higher activity due to the change of geometry of the 14VE complex leading to an easier dissociation. Because the $b/d$ ratio should be closely linked to the strength of the Pd−olefin bond (the more donating are the ligands, the stronger is the bond), we deduced from these data that complexes **2br** and **2dr** should display similar activities and should be less reactive than **2ar** and **2er** if the dissociation step is indeed the rate-determining step. On the other hand, considering our previous remark, complex **2cr** should be more active than **2br** and **2dr**. Therefore, to test the reliability of this method in predicting the reactivity of complexes, some competitive experiments were carried out.

**4. Competitive Catalytic Experiments.** The catalytic activity of allyl triflate complexes **1br**, **1cr**, **1dr**, and **1er** was evaluated in the allylation of aniline. Each experiment was conducted with 1 mol % of catalyst using 1 equiv of allylic alcohol and 2 equiv of amine. In line with theoretical predictions, the less active complexes are **1br** and **1dr**, which show similar activities. The most active catalyst is **1er**, and **1cr** exhibits an intermediate activity. Indeed, under mild conditions (1 h at room temperature), **1br** and **1dr** show no or very little activity, but interestingly heating at 50 °C for 24 h leads to similar conversions (20%). On the contrary, complex **1er** leads to a very good conversion in 1 h (76%).[19] As expected, complex **1cr** proved to be less reactive than **1er** but more active than **1br** and **1dr** (conversion of 47% in 1 h). These results are summarized in Table 3 (Scheme 26). CDA calculations are consistent with the observed reactivities. Nevertheless, **1er** displays a lower activity than the DPCB complex,[5] while they have similar $b/d$ ratios. This shows the limitations of this kind of CDA calculations at our computational level. Another interesting remark deals with the nature of the counteranion. Experiments were carried out with complex **1er** using either $TfO^-$ or $BF_4^-$ as counterions, and no reactivity difference was observed. However, it is clear that additional investigations are needed before concluding on the influence of the counteranion.

**5. Nature of the Substrate.** Having addressed ligands effects, we focused the end of our study on the nature of substrates. Indeed, methylamine was chosen as a model substrate for theoretical calculations to reduce computation time, but experiments were conducted with aniline. Therefore, the catalytic cycle was computed with aniline as substrate using the model complex **2a** (Scheme 27).

The first step is significantly affected by the nature of the substrate regarding the exothermicity of the reaction. The dissociation step of the olefin turns out to be more favored when

(19) $[Pd(P(OPh)_3)_4]$ has been used to convert aniline in harsher conditions, see: Kayaki, Y.; Koda, T.; Ikariya, T. *J. Org. Chem.* **2004**, *69*, 2595−2597.

***Scheme 28.*** Amination of Allyl Alcohol with **1er** Varying the Amine

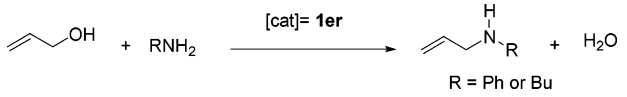


***Scheme 29.*** Proposed Catalytic Cycle

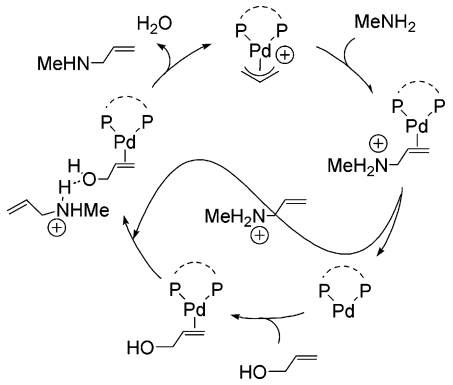


aniline is used as substrate ($\Delta E_{PCM}^{\ddagger} = 29.3$ kcal/mol for $MeNH_2$ and 21.0 kcal/mol for $PhNH_2$). The formation of the adduct is also much less exothermic for aniline. Finally, the last step is also favored in the case of aniline because it requires a weaker activation energy ($\Delta E_{PCM}^{\ddagger} = 21.7$ kcal/mol for $MeNH_2$ and 14.8 kcal/mol for $PhNH_2$). Note that the energetic profile of the last step is in good agreement with the respective basicity of the two amines, the $PhNH_2Me^+$ being less stable than $MeNH_2Me^+$ (aniline, $pK_a = 4.6$ and methylamine, $pK_a = 10.75$).

These calculations show that, while the reaction should proceed with aniline at room temperature, this should not be the case with methylamine given the activation energies needed. Experiments with our best catalyst (**1er**) were carried out. When *n*-butylamine is used as an example of alkylamine, no conversion was observed, even after 24 h at 50 °C, while a conversion of 76% after 1 h at room temperature with aniline as substrate was observed (Scheme 28).

## Conclusions

In this study, the mechanism of the allylation of primary amines was examined. Calculations show that two pathways are conceivable. The first one, which was recently proposed in the literature, relies on the formation of cationic Pd hydrido species. A mechanism, which formally involves a (1,3) palladium-assisted shift of a proton from the nitrogen to a carbon atom, has been proposed to rationalize their formation. In this context, it was also unambiguously shown that the existence of stable platinum complexes deriving from the corresponding hydrido species does not imply that palladium complexes should behave similarly. This can be traced to the remarkable ability of Pt(II) fragments to $\pi$-back-donate in the $\pi^*$-system of a coordinated olefin. The second mechanism, which bears resemblance to the currently admitted mechanism for allylic nucleophilic substitutions, involves the formation of a transient dicoordinated 14VE Pd(0) complex. This kind of intermediate has also been suggested by experimental observation made by Hartwig et al. (Scheme 29). Both mechanisms converge in the last step to an interesting intermolecular protonation process of the alcohol functionality by an ammonium, which yields the amine, water, and the allyl complex precursor. Much evidence favors the second mechanism. Indeed, the overall activation energy is lower for this mechanism, and only one high energetic state is involved. Moreover, among the highest energetic states involved in the first mechanism, the formation of the pentacoordinated 18VE Pd(II) complex is disfavored when the full substitution scheme of the ligand is considered.

The second mechanism is also fully consistent with both theoretical and experimental studies on the electronic influence of the ligands. This study highlights the fact that strong $\pi$-acceptor ligands favor the dissociation step, which is the rate-determining step. CDA calculations were correlated with competitive experiments and shown to be good probes to quantify the activity of a given palladium complex. Most interestingly, this mechanistic study led us to devise an efficient catalyst featuring a commercially available ligand, the strong $\pi$-acceptor triphenyl phosphite. Finally, we have shown that the nature of the amine also influences the overall process in facilitating both the decoordination of the allylammonium and the elimination of water to re-form the catalytic precursor in the case of aniline.[20] Further studies will now focus on the design of new catalysts employing mono- and bidentate strong $\pi$-acceptor ligands.

## Experimental Section

**General Remarks.** All reactions were routinely performed under an inert atmosphere of argon or nitrogen by using Schlenk and glovebox techniques and dry deoxygenated solvents. Dry THF and hexanes were obtained by distillation from Na/benzophenone. Dry dichloromethane was distilled from $P_2O_5$, and dry toluene was from Na. NMR spectra were recorded on a Bruker Avance 300 spectrometer operating at 300 MHz for $^1H$, 75.5 MHz for $^{13}C$, and 121.5 MHz for $^{31}P$. Solvent peaks are used as internal reference relative to $Me_4Si$ for $^1H$ and $^{13}C$ chemical shifts (ppm); $^{31}P$ chemical shifts are relative to a 85% $H_3PO_4$ external reference, and coupling constants are expressed in Hertz. The following abbreviations are used: b, broad; s, singlet; d, doublet; t, triplet; m, multiplet; p, pentuplet; sext, sextuplet; sept, septuplet; v, virtual. Elemental analyses were performed by the "Service d'analyze du CNRS", at Gif sur Yvette, France. Glyoxal-bis-(2,6-diisopropylphenyl)-imine (DAD)[21] and complex **1c**[22] were prepared according to literature procedures. All other reagents and chemicals were obtained commercially and used as received. The GC conversions were determined on a Varian Star 3400 gas chromatograph equipped with a CHROMPACK column (column type, WCOT FUSED SILICA; stationary phase, CP-SIL 5 CB).

**Theoretical Methods.** Calculations were performed with the Gaussian 03 series of programs.[23] Geometries were optimized using the B3PW91 functional.[24] The standard 6-31+G* basis set was used for all atoms (H, C, N, O, S, F, and P). The basis set used for metals (Pd

(20) During the reviewing process, one reviewer wisely mentioned that the presence of a certain amount of water can notably enhance the coupling process when DPCB ligands are employed (see: Murakami, H.; Minami, T.; Ozawa, F. *J. Org. Chem.* **2004**, *69*, 4482−4486). Additional calculations considering water as solvent using the PCM method were carried out to rationalize this observation. The main conclusion of these calculations is that increasing the polarity of the medium should result in a weaker activation energy for the dissociation step of the olefin ($\Delta E_{PCM}^{\ddagger} = +21.5$ kcal/mol for the conversion of **2a** into **12a** and $\Delta E_{PCM}^{\ddagger} = +31.4$ kcal/mol for the conversion of **2a** into **7a**). However, care must be taken because this coupling process was never carried out with water as the sole solvent. It was also previously shown that water is not crucial and the coupling process also proceeds with DPCB ligand even when $MgSO_4$ is present in the reaction medium as water scavenger (with lower reaction rates).

(21) Zettlitzer, M.; Tom Dieck, H.; Haupt, E. T. K.; Stamp, L. *Chem. Ber.* **1986**, *119*, 1868−1875.
(22) Amatore, C.; Jutand, A.; M'Barki, M. A.; Meyer, G.; Mottier, L. *Eur. J. Inorg. Chem.* **2001**, 873−880.
(23) Frisch, M. J.; et al. *Gaussian 03*, revision B.04; Gaussian, Inc.: Pitsburgh, PA, 2003.
(24) Becke, A. D. J. *J. Phys. Chem.* **1993**, *98*, 5648−5662. Perdew, J. P.; Wang, Y. *Phys. Rev. B* **1992**, *45*, 13244−13249.

and Pt) is the Hay and Wadt[25] small core quasirelativistic effective core potential with the double-$\zeta$ valence basis set (441s/2111p/311d for Pd and 441s/2111p/21d for Pt) augmented with an f-polarization function (exponent = 1.472 for Pd and exponent = 0.993 for Pt).[26] Minima and transition states were characterized by frequency calculations. Intrinsic reaction coordinates calculations (IRC) were performed to ensure that transition states connect the two concerned minima. Single point calculations were performed on all optimized geometries at the same level of theory as that used for optimizations using the PCM-UFF model.[27] The dielectric constant in the PCM calculations was set to $\epsilon = 7.58$ to simulate the THF solvent medium. ONIOM calculations were performed at the same level of theory for the QM part and using the UFF force field model[28] for the MM part of the molecule. Single point calculations were performed on ONIOM optimized geometries at the quantum level for all atoms using the PCM-UFF model (**1ar**, **2ar**, **8ar**, and **12ar**). Inspection of ligand to metal donor−acceptor interactions was performed using the charge-decomposition analysis (CDA);[17] the basis set for the metal was that associated with the pseudo potential, with a standard double-$\zeta$ LANL2DZ contraction.

**Acknowledgment.** The CNRS and the Ecole Polytechnique and the IDRIS (for computer time, project no. 061616) are thanked for supporting this work.

**Supporting Information Available:** Computed Cartesian coordinates, thermochemistry and PCM energies, three lower frequencies of all theoretical structures, and complete ref 23. Experimental procedures for the synthesis of complexes **1b**,**c**,**d**,**e** and general procedures for catalytic reactions. This material is available free of charge via the Internet at http://pubs.acs.org.

JA0621997

(25) Hay, P. J.; Wadt, W. R. *J. Chem. Phys.* **1985**, *82*, 299−310.
(26) Ehlers, A. W.; Bohme, M.; Dapprich, S.; Gobbi, A.; Hollwarth, A.; Jonas, V.; Kohler, K. F.; Stegmann, R.; Veldkamp, A.; Frenking, G. *Chem. Phys. Lett.* **1993**, *208*, 111−114.
(27) (a) Barone, V.; Improta, R.; Rega, N. *Theor. Chem. Acc.* **2004**, *111*, 237−245. (b) Cossi, M.; Scalmani, G.; Rega, N.; Barone, V. *J. Chem. Phys.* **2002**, *117*, 43−54. (c) Cossi, M.; Barone, V.; Cammi, R.; Tomasi, J. *Chem. Phys. Lett.* **1996**, *255*, 327−335. (d) Miertus, S.; Scrocco, E.; Tomasi, J. *Chem. Phys.* **1981**, *55*, 117−129.
(28) Rappe, A. K.; Casewit, C. J.; Colwell, K. S.; Goddard, W. A.; Skiff, W. M. *J. Am. Chem. Soc.* **1992**, *114*, 10024−10035.